

Stabilized Control Volume Finite Element Method for Drift-Diffusion

Kara Peterson

Pavel Bochev Mauro Perego Suzey Gao

Gary Hennigan Larry Musson

Sandia National Laboratories

UNM Applied Math Seminar

February 6, 2017

SAND2017-1293PE

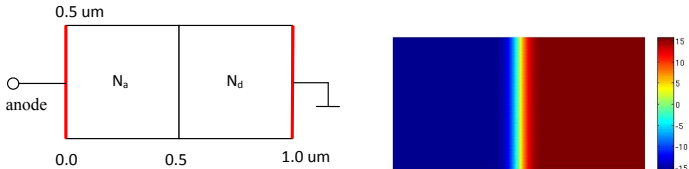


Sandia National Laboratories is a multi-mission laboratory managed and operated by Sandia Corporation, a wholly owned subsidiary of Lockheed Martin Corporation, for the U.S. Department of Energy's National Nuclear Security Administration under contract DE-AC04-94AL85000.

Outline

- 1 Introduction to CVFEM
- 2 Scharfetter-Gummel Upwinding
- 3 Stabilization with Multi-dimensional S-G Upwinding
- 4 Extension to FEM
- 5 Multi-scale Stabilized CVFEM
- 6 Conclusions

Motivation



Scaled coupled drift-diffusion equations for semi-conductors

$$\nabla \cdot (\lambda^2 \mathbf{E}) - (p - n + C) = 0 \quad \text{and} \quad \mathbf{E} = -\nabla\psi \quad \text{in } \Omega \times [0, T]$$

$$\frac{\partial n}{\partial t} - \nabla \cdot \mathbf{J}_n + R(\psi, n, p) = 0 \quad \text{and} \quad \mathbf{J}_n = \mu_n \mathbf{E} n + D_n \nabla n \quad \text{in } \Omega \times [0, T]$$

$$\frac{\partial p}{\partial t} + \nabla \cdot \mathbf{J}_p + R(\psi, n, p) = 0 \quad \text{and} \quad \mathbf{J}_p = \mu_p \mathbf{E} p - D_p \nabla p \quad \text{in } \Omega \times [0, T]$$

E - electric field n - electron density
 ψ - electric potential p - hole density

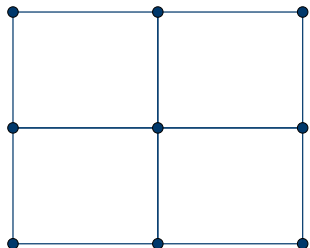
Want a numerical scheme that is accurate and stable in the strong drift regime

CVFEM Formulation

Electron continuity equation

$$\frac{\partial n}{\partial t} - \nabla \cdot \mathbf{J} + R = 0$$

$$\mathbf{J} = \mu \mathbf{E} n + D \nabla n$$



CVFEM Formulation

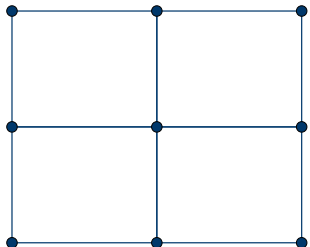
Electron continuity equation

$$\frac{\partial n}{\partial t} - \nabla \cdot \mathbf{J} + R = 0$$

$$\mathbf{J} = \mu \mathbf{E} n + D \nabla n$$

- Finite element approximation of the electron density

$$n^h(t, \mathbf{x}) = \sum_j n_j(t) \phi_j(\mathbf{x})$$



CVFEM Formulation

Electron continuity equation

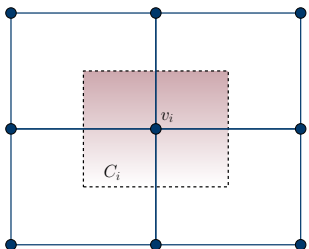
$$\frac{\partial n}{\partial t} - \nabla \cdot \mathbf{J} + R = 0$$

$$\mathbf{J} = \mu \mathbf{E} n + D \nabla n$$

- Finite element approximation of the electron density

$$n^h(t, \mathbf{x}) = \sum_j n_j(t) \phi_j(\mathbf{x})$$

- For each primary grid vertex, define a control volume

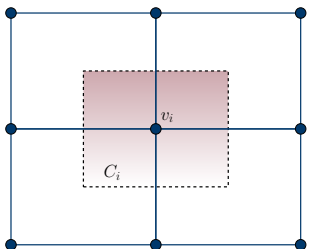


CVFEM Formulation

Electron continuity equation

$$\frac{\partial n}{\partial t} - \nabla \cdot \mathbf{J} + R = 0$$

$$\mathbf{J} = \mu \mathbf{E} n + D \nabla n$$



- Finite element approximation of the electron density
- $$n^h(t, \mathbf{x}) = \sum_j n_j(t) \phi_j(\mathbf{x})$$
- For each primary grid vertex, define a control volume
 - Integrate over the control volume and apply the divergence theorem

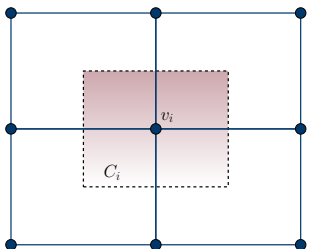
$$\int_{C_i} \frac{\partial n}{\partial t} dV - \int_{\partial C_i} \mathbf{J}(n) \cdot \vec{\mathbf{n}} dS + \int_{C_i} R(n), dV = 0$$

CVFEM Formulation

Electron continuity equation

$$\frac{\partial n}{\partial t} - \nabla \cdot \mathbf{J} + R = 0$$

$$\mathbf{J} = \mu \mathbf{E} n + D \nabla n$$



- Finite element approximation of the electron density

$$n^h(t, \mathbf{x}) = \sum_j n_j(t) \phi_j(\mathbf{x})$$

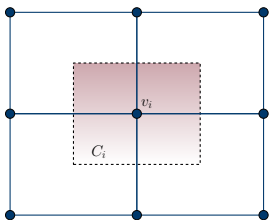
- For each primary grid vertex, define a control volume
- Integrate over the control volume and apply the divergence theorem

$$\int_{C_i} \frac{\partial n^h}{\partial t} dV - \int_{\partial C_i} \mathbf{J}(n^h) \cdot \vec{\mathbf{n}} dS + \int_{C_i} R(n^h) dV = 0$$

CVFEM Formulation

$$\int_{\partial C_i} \mathbf{J}(n^h) \cdot \vec{\mathbf{n}} \, dS = \sum_j n_j(t) \int_{\partial C_i} (\mu \mathbf{E} \phi_j + D \nabla \phi_j) \cdot \vec{\mathbf{n}} \, dS$$

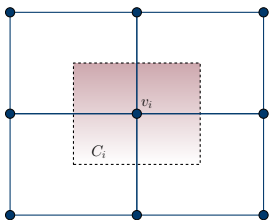
$$\mathbf{K}_{ij} = \int_{\partial C_i} (\mu \mathbf{E} \phi_j + D \nabla \phi_j) \cdot \vec{\mathbf{n}} \, dS$$



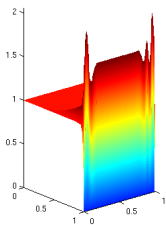
CVFEM Formulation

$$\int_{\partial C_i} \mathbf{J}(n^h) \cdot \vec{\mathbf{n}} \, dS = \sum_j n_j(t) \int_{\partial C_i} (\mu \mathbf{E} \phi_j + D \nabla \phi_j) \cdot \vec{\mathbf{n}} \, dS$$

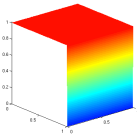
$$\mathbf{K}_{ij} = \int_{\partial C_i} (\mu \mathbf{E} \phi_j + D \nabla \phi_j) \cdot \vec{\mathbf{n}} \, dS$$



In strong drift regime this formulation can result in instabilities



Unstabilized CVFEM

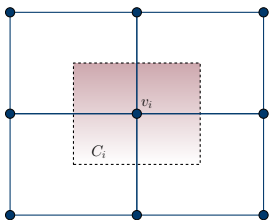


Correct Solution

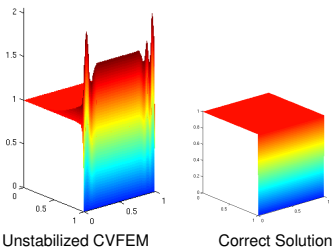
CVFEM Formulation

$$\int_{\partial C_i} \mathbf{J}(n^h) \cdot \vec{\mathbf{n}} \, dS = \sum_j n_j(t) \int_{\partial C_i} (\mu \mathbf{E} \phi_j + D \nabla \phi_j) \cdot \vec{\mathbf{n}} \, dS$$

$$\mathbf{K}_{ij} = \int_{\partial C_i} (\mu \mathbf{E} \phi_j + D \nabla \phi_j) \cdot \vec{\mathbf{n}} \, dS$$



In strong drift regime this formulation can result in instabilities



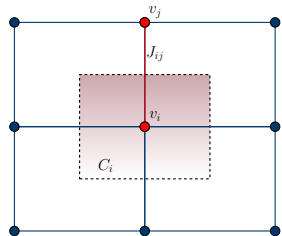
Want an approximation $\mathbf{J}(n^h) \cdot \vec{\mathbf{n}}$ that includes information about the drift

Scharfetter-Gummel Upwinding

*On edge e_{ij} solve 1-d boundary value problem
along edge for constant J_{ij}*

$$\frac{dJ_{ij}}{ds} = 0; \quad J_{ij} = \mu E_{ij} n(s) + D \frac{dn(s)}{ds}$$

$$n(0) = n_i \quad \text{and} \quad n(h_{ij}) = n_j$$



D. L. Scharfetter and H. K Gummel, Large-signal analysis of a silicon read diode oscillator, *IEEE Transactions on Electron Devices* 16, 64-77, 1969.

Scharfetter-Gummel Upwinding

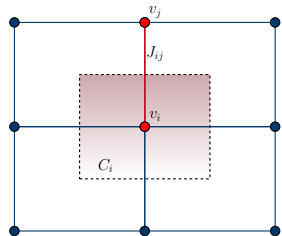
*On edge e_{ij} solve 1-d boundary value problem
along edge for constant J_{ij}*

$$\frac{dJ_{ij}}{ds} = 0; \quad J_{ij} = \mu E_{ij} n(s) + D \frac{dn(s)}{ds}$$

$$n(0) = n_i \quad \text{and} \quad n(h_{ij}) = n_j$$

$$J_{ij} = \frac{a_{ij} D_n}{h_{ij}} (n_j (\coth(a_{ij}) + 1) - n_i (\coth(a_{ij}) - 1))$$

$$\text{where } a_{ij} = \frac{h_{ij} E_{ij} \mu}{2D}, \quad E_{ij} = -\frac{(\psi_j - \psi_i)}{h_{ij}}$$



D. L. Scharfetter and H. K Gummel, Large-signal analysis of a silicon read diode oscillator, *IEEE Transactions on Electron Devices* 16, 64-77, 1969.

Scharfetter-Gummel Upwinding

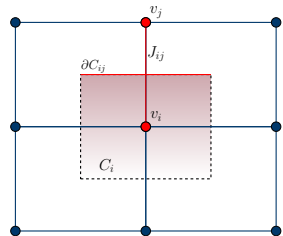
*On edge e_{ij} solve 1-d boundary value problem
along edge for constant J_{ij}*

$$\frac{dJ_{ij}}{ds} = 0; \quad J_{ij} = \mu E_{ij} n(s) + D \frac{dn(s)}{ds}$$

$$n(0) = n_i \quad \text{and} \quad n(h_{ij}) = n_j$$

$$J_{ij} = \frac{a_{ij} D_n}{h_{ij}} (n_j (\coth(a_{ij}) + 1) - n_i (\coth(a_{ij}) - 1))$$

$$\text{where } a_{ij} = \frac{h_{ij} E_{ij} \mu}{2D}, \quad E_{ij} = -\frac{(\psi_j - \psi_i)}{h_{ij}}$$



$$\int_{\partial C_i} \mathbf{J}_n \cdot \bar{\mathbf{n}} dS \approx \sum_{\partial C_{ij} \in \partial C_i} J_{ij} |\partial C_{ij}|$$

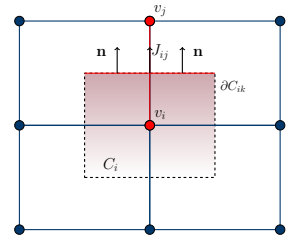
D. L. Scharfetter and H. K Gummel, Large-signal analysis of a silicon read diode oscillator, *IEEE Transactions on Electron Devices* 16, 64-77, 1969.

Scharfetter-Gummel Upwinding

On edge e_{ij} solve 1-d boundary value problem along edge for constant J_{ij}

$$\frac{dJ_{ij}}{ds} = 0; \quad J_{ij} = \mu E_{ij} n(s) + D \frac{dn(s)}{ds}$$

$$n(0) = n_i \quad \text{and} \quad n(h_{ij}) = n_j$$



$$J_{ij} = \frac{a_{ij} D_n}{h_{ij}} (n_j (\coth(a_{ij}) + 1) - n_i (\coth(a_{ij}) - 1))$$

$$\text{where } a_{ij} = \frac{h_{ij} E_{ij} \mu}{2D}, \quad E_{ij} = -\frac{(\psi_j - \psi_i)}{h_{ij}}$$

On structured grids, J_{ij} is a good estimate of $\mathbf{J} \cdot \vec{\mathbf{n}}$ on ∂C_{ij}

$$\int_{\partial C_i} \mathbf{J}_n \cdot \vec{\mathbf{n}} dS \approx \sum_{\partial C_{ij} \in \partial C_i} J_{ij} |\partial C_{ij}|$$

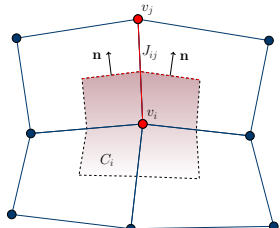
D. L. Scharfetter and H. K Gummel, Large-signal analysis of a silicon read diode oscillator, *IEEE Transactions on Electron Devices* 16, 64-77, 1969.

Scharfetter-Gummel Upwinding

On edge e_{ij} solve 1-d boundary value problem along edge for constant J_{ij}

$$\frac{dJ_{ij}}{ds} = 0; \quad J_{ij} = \mu E_{ij} n(s) + D \frac{dn(s)}{ds}$$

$n(0) = n_i \quad \text{and} \quad n(h_{ij}) = n_j$



$$J_{ij} = \frac{a_{ij} D_n}{h_{ij}} (n_j (\coth(a_{ij}) + 1) - n_i (\coth(a_{ij}) - 1))$$

where $a_{ij} = \frac{h_{ij} E_{ij} \mu}{2D}$, $E_{ij} = -\frac{(\psi_j - \psi_i)}{h_{ij}}$

On unstructured grids, J_{ij} is no longer a good estimate of $\mathbf{J} \cdot \vec{\mathbf{n}}$

$$\int_{\partial C_i} \mathbf{J}_n \cdot \vec{\mathbf{n}} dS \approx \sum_{\partial C_{ij} \in \partial C_i} J_{ij} |\partial C_{ij}|$$

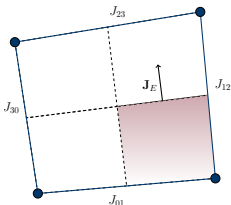
D. L. Scharfetter and H. K Gummel, Large-signal analysis of a silicon read diode oscillator, *IEEE Transactions on Electron Devices* 16, 64-77, 1969.

Multi-dimensional S-G Upwinding

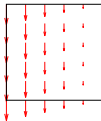
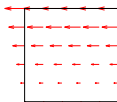
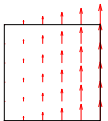
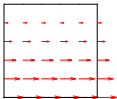
Idea: Use $H(\text{curl})$ -conforming finite elements to expand edge currents into primary cell

Exponentially fitted current density

$$\mathbf{J}_E(\mathbf{x}) = \sum_{e_{ij}} h_{ij} J_{ij} \vec{W}_{ij}(\mathbf{x})$$



$$\int_{e_{ij}} \vec{W}_{ij} \cdot \mathbf{t}_{rs} dl = \delta_{ij}^{rs}$$



$$\vec{W}_{01} = \left(\frac{1-y}{4}, 0 \right) \quad \vec{W}_{12} = \left(0, \frac{1+x}{4} \right) \quad \vec{W}_{23} = \left(-\frac{1+y}{4}, 0 \right) \quad \vec{W}_{30} = \left(0, -\frac{1-x}{4} \right)$$

P. Bochev, K. Peterson, X. Gao A new control-volume finite element method for the stable and accurate solution of the drift-diffusion equations on general unstructured grids, *CMAME*, 254, pp. 126-145, 2013.

Multi-dimensional S-G Upwinding

Exponentially fitted current density

$$\mathbf{J}_E(\mathbf{x}) = \sum_{e_{ij}} h_{ij} J_{ij} \vec{W}_{ij}(\mathbf{x})$$

Nodal space, $\mathbf{G}_D^h(\Omega)$, and edge element space, $\mathbf{C}_D^h(\Omega)$, belong to an exact sequence

given $\phi_i \in \mathbf{G}_D^h(\Omega)$, then $\nabla \phi_i \in \mathbf{C}_D^h(\Omega)$

For the lowest order case

$$\nabla \phi_i = \sum_{e_{ij} \in E(v_i)} \sigma_{ij} \vec{W}_{ij}, \quad \sigma_{ij} = \pm 1$$

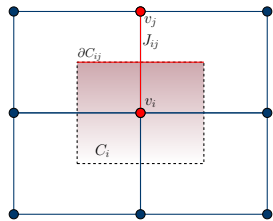
If the carrier drift velocity $\mu \mathbf{E} = 0$, $J_{ij} = \frac{D(n_j - n_i)}{h_{ij}}$

$$\mathbf{J}_E = \sum_{e_{ij} \in E(\Omega)} D(n_j - n_i) \vec{W}_{ij} = \sum_{v_i \in V(\Omega)} D n_j \nabla \phi_j = \mathbf{J}(n^h)$$

Multi-dimensional S-G Upwinding

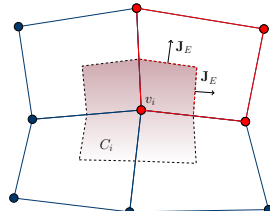
Standard S-G

$$\int_{\partial C_i} \mathbf{J} \cdot \vec{\mathbf{n}} dS \approx \sum_{\partial C_{ij} \in \partial C_i} J_{ij} |\partial C_{ij}|$$



Multi-dimensional S-G

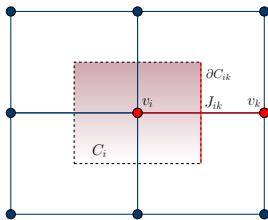
$$\int_{\partial C_i} \mathbf{J} \cdot \vec{\mathbf{n}} dS \approx \sum_{\partial C_{ij}^K \in \partial C_i} \mathbf{J}_E \cdot \vec{\mathbf{n}} |\partial C_{ij}^K|$$



Multi-dimensional S-G Upwinding

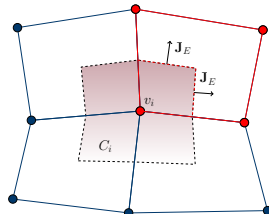
Standard S-G

$$\int_{\partial C_i} \mathbf{J} \cdot \vec{\mathbf{n}} dS \approx \sum_{\partial C_{ij} \in \partial C_i} J_{ij} |\partial C_{ij}|$$



Multi-dimensional S-G

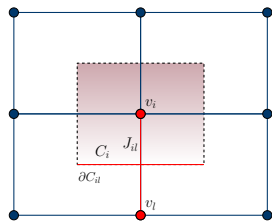
$$\int_{\partial C_i} \mathbf{J} \cdot \vec{\mathbf{n}} dS \approx \sum_{\partial C_{ij}^K \in \partial C_i} \mathbf{J}_E \cdot \vec{\mathbf{n}} |\partial C_{ij}^K|$$



Multi-dimensional S-G Upwinding

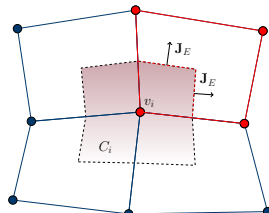
Standard S-G

$$\int_{\partial C_i} \mathbf{J} \cdot \vec{\mathbf{n}} dS \approx \sum_{\partial C_{ij} \in \partial C_i} J_{ij} |\partial C_{ij}|$$



Multi-dimensional S-G

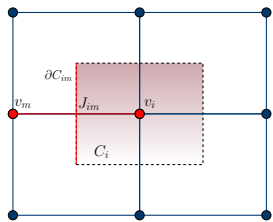
$$\int_{\partial C_i} \mathbf{J} \cdot \vec{\mathbf{n}} dS \approx \sum_{\partial C_{ij}^K \in \partial C_i} \mathbf{J}_E \cdot \vec{\mathbf{n}} |\partial C_{ij}^K|$$



Multi-dimensional S-G Upwinding

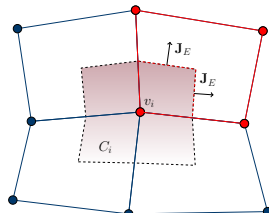
Standard S-G

$$\int_{\partial C_i} \mathbf{J} \cdot \vec{\mathbf{n}} dS \approx \sum_{\partial C_{ij} \in \partial C_i} J_{ij} |\partial C_{ij}|$$



Multi-dimensional S-G

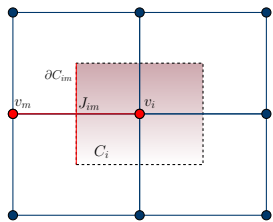
$$\int_{\partial C_i} \mathbf{J} \cdot \vec{\mathbf{n}} dS \approx \sum_{\partial C_{ij}^K \in \partial C_i} \mathbf{J}_E \cdot \vec{\mathbf{n}} |\partial C_{ij}^K|$$



Multi-dimensional S-G Upwinding

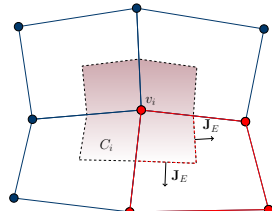
Standard S-G

$$\int_{\partial C_i} \mathbf{J} \cdot \vec{\mathbf{n}} dS \approx \sum_{\partial C_{ij} \in \partial C_i} J_{ij} |\partial C_{ij}|$$



Multi-dimensional S-G

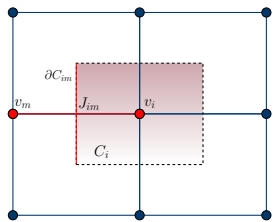
$$\int_{\partial C_i} \mathbf{J} \cdot \vec{\mathbf{n}} dS \approx \sum_{\partial C_{ij}^K \in \partial C_i} \mathbf{J}_E \cdot \vec{\mathbf{n}} |\partial C_{ij}^K|$$



Multi-dimensional S-G Upwinding

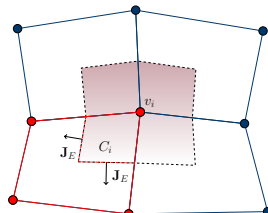
Standard S-G

$$\int_{\partial C_i} \mathbf{J} \cdot \vec{\mathbf{n}} dS \approx \sum_{\partial C_{ij} \in \partial C_i} J_{ij} |\partial C_{ij}|$$



Multi-dimensional S-G

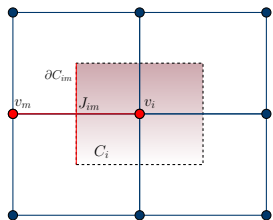
$$\int_{\partial C_i} \mathbf{J} \cdot \vec{\mathbf{n}} dS \approx \sum_{\partial C_{ij}^K \in \partial C_i} \mathbf{J}_E \cdot \vec{\mathbf{n}} |\partial C_{ij}^K|$$



Multi-dimensional S-G Upwinding

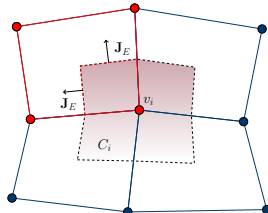
Standard S-G

$$\int_{\partial C_i} \mathbf{J} \cdot \vec{\mathbf{n}} dS \approx \sum_{\partial C_{ij} \in \partial C_i} J_{ij} |\partial C_{ij}|$$



Multi-dimensional S-G

$$\int_{\partial C_i} \mathbf{J} \cdot \vec{\mathbf{n}} dS \approx \sum_{\partial C_{ij}^K \in \partial C_i} \mathbf{J}_E \cdot \vec{\mathbf{n}} |\partial C_{ij}^K|$$



Manufactured Solution on Structured Grid

Steady-state manufactured solution

$$\begin{aligned} -\nabla \cdot \mathbf{J} + R &= 0 \quad \text{in } \Omega \\ n = g &\quad \text{on } \Gamma_D \end{aligned}$$

$$\begin{aligned} n(x, y) &= x^3 - y^2 \\ \mu \mathbf{E} &= (-\sin \pi/6, \cos \pi/6) \end{aligned}$$

	CVFEM-SG		FVM-SG	
	L^2 error	H^1 error	L^2 error	H^1 error
Grid	$D = 1 \times 10^{-3}$			
32	0.4373E-02	0.7620E-01	0.4364E-02	0.7572E-01
64	0.2108E-02	0.4954E-01	0.2107E-02	0.4937E-01
128	0.9870E-03	0.3089E-01	0.9870E-03	0.3084E-01
Rate	1.095	0.681	1.094	0.679
Grid	$D = 1 \times 10^{-5}$			
32	0.4732E-02	0.7897E-01	0.4723E-02	0.7850E-01
64	0.2517E-02	0.5477E-01	0.2515E-02	0.5460E-01
128	0.1298E-02	0.3834E-01	0.1298E-02	0.3828E-01
Rate	0.955	0.514	0.955	0.514

CVFEM-SG control volume finite element method with multi-dimensional S-G upwinding
 FVM-SG finite volume method with 1-d S-G upwinding

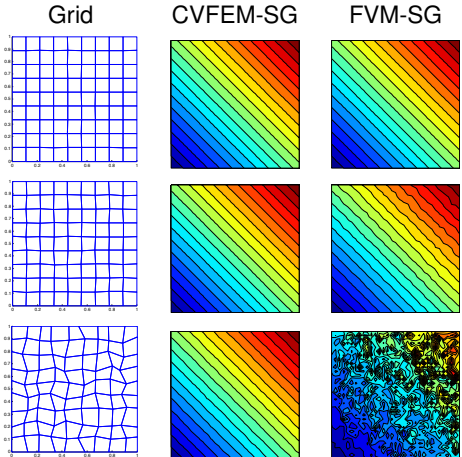
Robustness on Unstructured Grids

Manufactured solution on randomly perturbed grids

$$\begin{aligned} -\nabla \cdot \mathbf{J} + R &= 0 \quad \text{in } \Omega \\ n = g \quad \text{on } \Gamma_D \end{aligned}$$

$$\begin{aligned} n(x, y) &= x + y \\ \mu \mathbf{E} &= (-\sin \pi/6, \cos \pi/6) \\ D &= 1.0 \times 10^{-5} \end{aligned}$$

Grid	Error	CVFEM-SG	FVM-SG
$O(h^2)$	L^2	0.88047E-06	0.83467E-04
	H^1	0.14524E-03	0.13426E-01
$O(h)$	L^2	0.38594E-04	0.36687E-02
	H^1	0.65073E-02	0.58993E+00
$O(1)$	L^2	0.21849E-02	0.24247E+00
	H^1	0.36473E+00	0.38469E+02



Charon

To solve coupled drift-diffusion equations CVFEM-SG has been implemented in Sandia's Charon code

- Electrical transport simulation code for semiconductor devices, solving PDE-based nonlinear equations
- Built with Trilinos libraries (<https://github.com/trilinos/Trilinos>) that provide
 - Framework and residual-based assembly (Panzer, Phalanx)
 - Linear and Nonlinear solvers (Belos, Nox, ML, etc)
 - Temporal and spatial discretization (Tempus, Intrepid, Shards)
 - Automatic differentiation (Sacado)
 - Advanced manycore performance portability (Kokkos)



CHARON



Trilinos

PN Diode

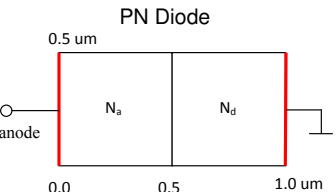
PN Diode coupled drift-diffusion equations

$$\nabla \cdot (\epsilon_0 \epsilon_{si} \nabla \psi) = -q(p - n + N_d - N_a) \quad \text{in } \Omega$$

$$-\nabla \cdot \mathbf{J}_n + R(\psi, n, p) = 0 \quad \text{in } \Omega$$

$$\nabla \cdot \mathbf{J}_p + R(\psi, n, p) = 0 \quad \text{in } \Omega$$

$$R(\psi, n, p) = \frac{np - n_i^2}{\tau_p(n+n_i) + \tau_n(p+n_i)} + (c_n n + c_p p)(np - n_i^2)$$



Compare with Streamlined Upwind Petrov-Galerkin(SUPG) method

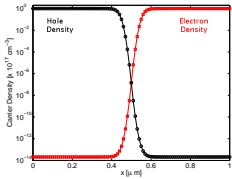
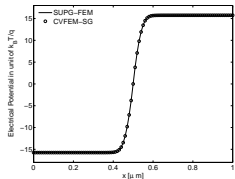
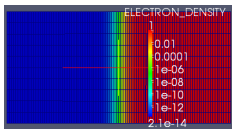
$$\int_{\Omega} (\mu \mathbf{E} + D \nabla n) \cdot \nabla \psi dV + \int_{\Omega} R \psi dV + \int_{\Omega} \tau (\mu \mathbf{E} \cdot \nabla n) (\mu \mathbf{E} \cdot \nabla \psi) dV = 0$$

τ - a parameter that depends on mesh size and velocity

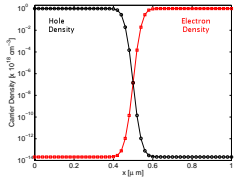
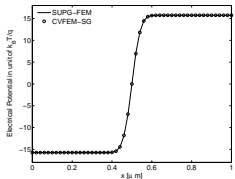
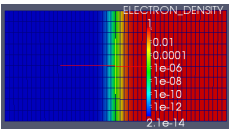
PN Diode

Mesh Dependence Study

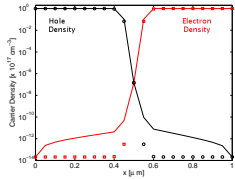
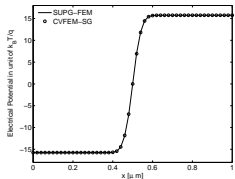
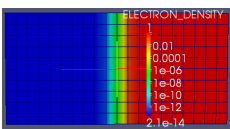
$$h_x = 0.01\mu m$$



$$h_x = 0.02\mu m$$



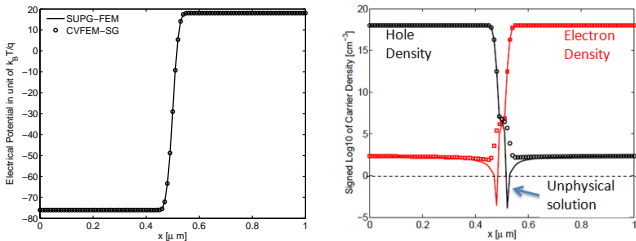
$$h_x = 0.05\mu m$$



PN Diode

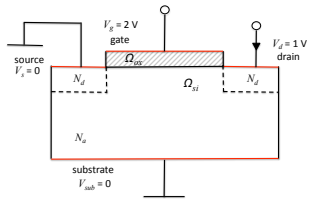
Strong Drift Case

$$N_a = N_d = 1.0 \times 10^{18} \text{ cm}^{-3}, \quad V_a = -1.5V$$



FEM-SUPG solution develops undershoots and becomes negative in junction region, while CVFEM-SG exhibits only minimal undershoots and values remain positive.

N-Channel MOSFET



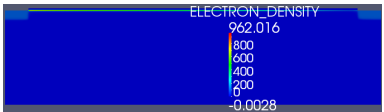
MOSFET coupled drift-diffusion equations

$$\nabla \cdot (\epsilon_0 \epsilon_{ox} \nabla \psi) = 0 \quad \text{in } \Omega_{ox}$$

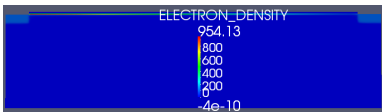
$$\nabla \cdot (\epsilon_0 \epsilon_{si} \nabla \psi) = -q \left(n_i \exp \left(\frac{-q\psi}{k_B T} \right) - n + N_d - N_a \right) \quad \text{in } \Omega_{si}$$

$$\nabla \cdot (n \mu_n \nabla \psi - D_n \nabla n) = 0 \quad \text{in } \Omega_{si}$$

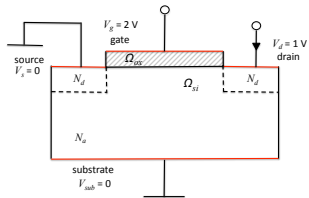
FEM-SUPG



CVFEM-SG



N-Channel MOSFET



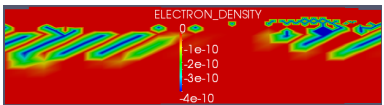
MOSFET coupled drift-diffusion equations

$$\nabla \cdot (\epsilon_0 \epsilon_{ox} \nabla \psi) = 0 \quad \text{in } \Omega_{ox}$$

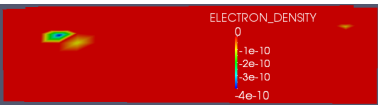
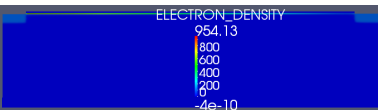
$$\nabla \cdot (\epsilon_0 \epsilon_{si} \nabla \psi) = -q \left(n_i \exp \left(\frac{-q\psi}{k_B T} \right) - n + N_d - N_a \right) \quad \text{in } \Omega_{si}$$

$$\nabla \cdot (n \mu_n \nabla \psi - D_n \nabla n) = 0 \quad \text{in } \Omega_{si}$$

FEM-SUPG



CVFEM-SG



FEM-SUPG solution exhibits larger negative values over a wider area than the CVFEM-SG solution.

Stabilization for FEM

Weak form of equation

$$\int_{\Omega} \frac{\partial n}{\partial t} \psi dV + \int_{\Omega} \mathbf{J} \cdot \nabla \psi dV + \int_{\Omega} R \psi dV = 0$$

Semi-discrete equation with stabilization

$$\int_{\Omega} \frac{\partial n^h}{\partial t} \psi dV + \int_{\Omega} \mathbf{J}_E(n^h) \cdot \nabla \psi dV + \int_{\Omega} R(n^h) \psi dV = 0$$

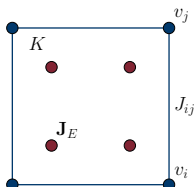
where

$$\mathbf{J}_E(\mathbf{x}) = \sum_{e_{ij}} h_{ij} J_{ij} \vec{W}_{ij}(\mathbf{x})$$

Electron continuity equation

$$\frac{\partial n}{\partial t} - \nabla \cdot \mathbf{J} + R = 0$$

$$\mathbf{J} = \mu \mathbf{E} n + D \nabla n$$



P. Bochev, K. Peterson, A parameter-free stabilized finite element method for scalar advection-diffusion problems, *Central European Journal of Mathematics*, Vol. 11, issue 8, pp. 1458-1477 (2013)

Symmetrized Stabilization for FEM

Consider the stabilized flux

$$\mathbf{J}_E(\mathbf{x}) = \sum_{e_{ij}} h_{ij} J_{ij} \vec{W}_{ij}(\mathbf{x})$$

It can be divided into a projection of the nodal flux and a stabilization term

Electron continuity equation

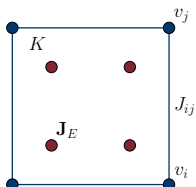
$$\frac{\partial n}{\partial t} - \nabla \cdot \mathbf{J} + R = 0$$

$$\mathbf{J} = \mu \mathbf{E} n + D \nabla n$$

$$\mathbf{J}_E(\mathbf{x}) = \mathcal{I}_E \left(\mu \mathbf{E} n^h + D \nabla n^h \right) + \Theta(n^h)$$

where

$$\mathcal{I}_E(\mathbf{u}) = \sum_{e_{ij} \in E(\Omega)} \vec{W}_{ij} \int_{e_{ij}} \mathbf{u} \cdot \mathbf{t}_{ij} dl$$



$$\Theta(n^h) = \sum_{e_{ij}} (n_j - n_i) \theta_{ij} \vec{W}_{ij}(\mathbf{x}), \quad \theta_{ij} = D (a_{ij} \coth(a_{ij}) - 1), \quad a_{ij} = \frac{\mu \mathbf{E} h_{ij}}{2D}$$

P. Bochev, M. Perego, K. Peterson, Formulation and analysis of a parameter-free stabilized finite element method, SINUM Vol. 53, No. 5, pp. 2363-2388 (2015).

Symmetrized Stabilization for FEM

Can use the stabilization term with the original nodal flux

$$\int_{\Omega} \left(\mu \mathbf{E} n^h + D \nabla n^h \right) \cdot \nabla \psi dV + \int_{\Omega} \Theta(n^h) \nabla \psi dV = 0$$

This form resembles a nonsymmetric artificial diffusion, which motivates the following symmetrized form

$$\int_{\Omega} \widehat{\Theta}(n^h) \cdot \widehat{\Theta}(\psi) dV = 0$$

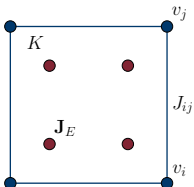
where

$$\widehat{\Theta}(n^h) = \sum_{e_{ij} \in E(\Omega)} (n_j - n_i) \sqrt{\theta_{ij}} \vec{W}_{ij}(\mathbf{x})$$

Electron continuity equation

$$\frac{\partial n}{\partial t} - \nabla \cdot \mathbf{J} + R = 0$$

$$\mathbf{J} = \mu \mathbf{E} n + D \nabla n$$



Symmetrized form has same accuracy (first-order in strong drift regime), but better stability

Symmetrized Stabilization for FEM

Stabilizing kernel automatically adjusts strength of artificial edge diffusion

Electron continuity equation

$$\theta_{ij} = D (\alpha_{ij} \coth(\alpha_{ij}) - 1)$$

In the diffusion limit

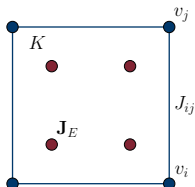
$$\lim_{\alpha_{ij} \rightarrow 0} \theta_{ij} = 0$$

In the drift limit

$$\lim_{\alpha_{ij} \rightarrow \infty} \theta_{ij} = \frac{h_{ij}}{2} |\mu \mathbf{E}|$$

$$\frac{\partial n}{\partial t} - \nabla \cdot \mathbf{J} + R = 0$$

$$\mathbf{J} = \mu \mathbf{E} n + D \nabla n$$



Manufactured Solution

D = 0.1

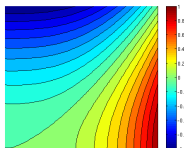
Grid	Quadrilaterals		Triangles	
	$\ \phi - \phi_h\ _0$	$\ \nabla\phi - \nabla\phi_h\ _0$	$\ \phi - \phi_h\ _0$	$\ \nabla\phi - \nabla\phi_h\ _0$
32	0.2437E-03	0.3609E-01	0.3623E-03	0.3610E-01
64	0.6099E-04	0.1804E-01	0.9093E-04	0.1804E-01
128	0.1525E-04	0.9021E-02	0.2275E-04	0.9021E-02
256	0.3813E-05	0.4511E-02	0.5690E-05	0.4511E-02
Rate	2.000	1.000	1.998	1.000

D = 0.001

Grid	Quadrilaterals		Triangles	
	$\ \phi - \phi_h\ _0$	$\ \nabla\phi - \nabla\phi_h\ _0$	$\ \phi - \phi_h\ _0$	$\ \nabla\phi - \nabla\phi_h\ _0$
32	0.4262E-02	0.7536E-01	0.7703E-02	0.8802E-01
64	0.2082E-02	0.4932E-01	0.3714E-02	0.5604E-01
128	0.9820E-03	0.3081E-01	0.1544E-02	0.3245E-01
256	0.3910E-03	0.1505E-01	0.5566E-03	0.1594E-01
Rate	1.276	0.934	1.375	0.951

D = 0.00001

Grid	Quadrilaterals		Triangles	
	$\ \phi - \phi_h\ _0$	$\ \nabla\phi - \nabla\phi_h\ _0$	$\ \phi - \phi_h\ _0$	$\ \nabla\phi - \nabla\phi_h\ _0$
32	0.4741E-02	0.7949E-01	0.8545E-02	0.9514E-01
64	0.2518E-02	0.5497E-01	0.4616E-02	0.6664E-01
128	0.1298E-02	0.3842E-01	0.2401E-02	0.4684E-01
256	0.6574E-03	0.2695E-01	0.1222E-02	0.3293E-01
Rate	0.964	0.517	0.952	0.510



$$\begin{aligned} -\nabla \cdot J(n) &= f \\ J(n) &= (D\nabla n - \mu E n) \end{aligned}$$

$$\begin{aligned} \phi(x, y) &= x^3 - y^2 \\ \mu E &= (-\sin(\pi/6), \cos(\pi/6)) \end{aligned}$$

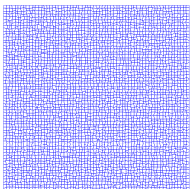
Double Glazing Test

$$\begin{aligned} -\nabla \cdot J(n) &= R && \text{in } \Omega \\ J(n) &= (D\nabla n + \mu \mathbf{E} n) && \text{in } \Omega \\ n &= g && \text{on } \Gamma \end{aligned}$$

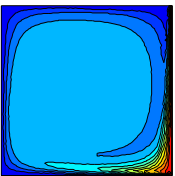
$$D = 0.00001 \quad \mu \mathbf{E} = \begin{pmatrix} 2(2y-1)(1-(2x-1)^2) \\ -2(2x-1)(1-(2y-1)^2) \end{pmatrix}$$

Random quadrilateral grid

Mesh



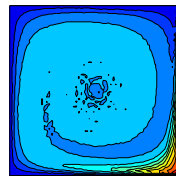
Symmetric Formulation



min = -0.1649

max = 1.0514

Original Formulation



min = -0.2644

max = 1.0956

Double Glazing Test

$$\begin{aligned} -\nabla \cdot J(n) &= R && \text{in } \Omega \\ J(n) &= (D\nabla n + \mu \mathbf{E} n) && \text{in } \Omega \\ n &= g && \text{on } \Gamma \end{aligned}$$

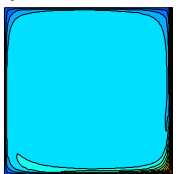
$$g = \begin{cases} 0 & \text{on } \Gamma_L \cup \Gamma_T \cup (\Gamma_B \cap \{x \leq 0.5\}) \\ 1 & \text{on } \Gamma_R \cup (\Gamma_B \cap \{x > 0.5\}) \end{cases}$$

$$D = 0.00001$$

$$\mu \mathbf{E} = \begin{pmatrix} 2(2y-1)(1-(2x-1)^2) \\ -2(2x-1)(1-(2y-1)^2) \end{pmatrix}$$

Uniform quadrilateral grid

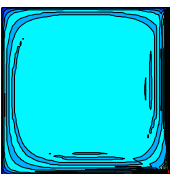
Symmetric Formulation



min = -0.0691

max = 1.0

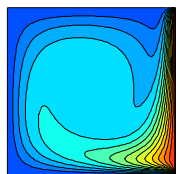
SUPG



min = -0.1494

max = 1.0

Artificial Diffusion



min = 0.0

max = 1.0

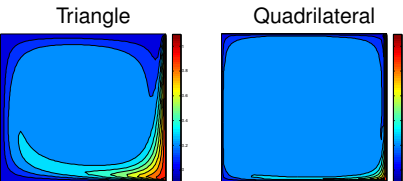
Double Glazing Test

$$\begin{aligned} -\nabla \cdot J(n) &= R && \text{in } \Omega \\ J(n) &= (D\nabla n + \mu \mathbf{E} n) && \text{in } \Omega \\ n &= g && \text{on } \Gamma \end{aligned}$$

$$g = \begin{cases} 0 & \text{on } \Gamma_L \cup \Gamma_T \cup (\Gamma_B \cap \{x \leq 0.5\}) \\ 1 & \text{on } \Gamma_R \cup (\Gamma_B \cap \{x > 0.5\}) \end{cases}$$

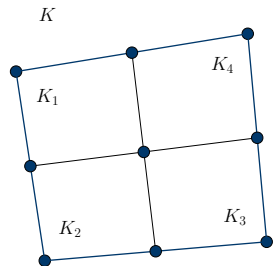
$$D = 0.00001 \quad \mu \mathbf{E} = \begin{pmatrix} 2(2y-1)(1-(2x-1)^2) \\ -2(2x-1)(1-(2y-1)^2) \end{pmatrix}$$

Stability estimate implies method is more diffusive on triangles



Multi-scale Stabilized CVFEM

*Divide each element into four
sub-elements*



Bochev, Peterson, Perego "A multi-scale control-volume finite element method for advection-diffusion equations", IJNMF Vol. 77, Issue 11, pp. 641-667 (2015).

Multi-scale Stabilized CVFEM

- Solve 1-d boundary value problem along a macro-element edge for a linear $J(s) = a + bs$

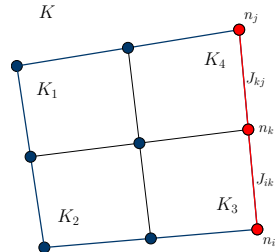
Divide each element into four

sub-elements

$$J(s) = \mu \mathbf{E}_s n(s) + D \frac{dn}{ds}$$

$$n(0) = n_i, \quad n(h_s/2) = n_k \quad \text{and} \quad n(h_s) = n_j$$

$$J_{ik} = J(h_s/4) \quad J_{kj} = J(3h_s/4)$$



Bochev, Peterson, Perego "A multi-scale control-volume finite element method for advection-diffusion equations", IJNMF Vol. 77, Issue 11, pp. 641-667 (2015).

Multi-scale Stabilized CVFEM

- Solve 1-d boundary value problem along a macro-element edge for a linear $J(s) = a + bs$

Divide each element into four

sub-elements

$$J(s) = \mu \mathbf{E}_s n(s) + D \frac{dn}{ds}$$

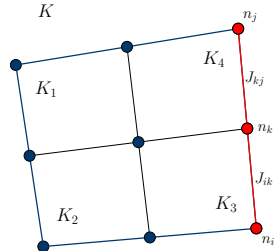
$$n(0) = n_i, \quad n(h_s/2) = n_k \quad \text{and} \quad n(h_s) = n_j$$

$$J_{ik} = J(h_s/4) \quad J_{kj} = J(3h_s/4)$$

- Edge flux

$$J_{ik} = J_{ik}^{1st}(n_i, n_k) + \gamma_{ik}(n_i, n_j, n_k)$$

$$J_{kj} = J_{kj}^{1st}(n_k, n_j) + \gamma_{kj}(n_i, n_j, n_k)$$



Bochev, Peterson, Perego "A multi-scale control-volume finite element method for advection-diffusion equations", IJNMF Vol. 77, Issue 11, pp. 641-667 (2015).

Multi-scale Stabilized CVFEM

- Solve 1-d boundary value problem along a macro-element edge for a linear $J(s) = a + bs$

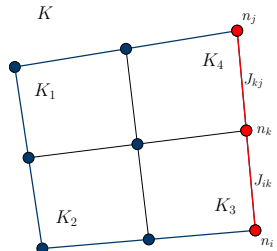
Divide each element into four

$$J(s) = \mu \mathbf{E}_s n(s) + D \frac{dn}{ds}$$

$$n(0) = n_i, \quad n(h_s/2) = n_k \quad \text{and} \quad n(h_s) = n_j$$

$$J_{ik} = J(h_s/4) \quad J_{kj} = J(3h_s/4)$$

sub-elements



- Edge flux

$$J_{ik} = J_{ik}^{1st}(n_i, n_k) + \gamma_{ik}(n_i, n_j, n_k)$$

$$J_{kj} = J_{kj}^{1st}(n_k, n_j) + \gamma_{kj}(n_i, n_j, n_k)$$

- Expand into primary (macro) cell using $H(\text{curl})$ -conforming finite elements

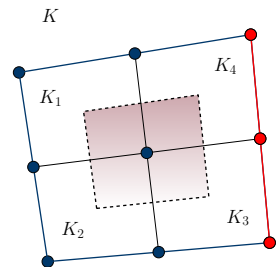
$$\mathbf{J}_E(n_h) = \sum_{e_{ij} \in E(\Omega)} J_{ij} \vec{W}_{ij}$$

Bochev, Peterson, Perego "A multi-scale control-volume finite element method for advection-diffusion equations", IJNMF Vol. 77, Issue 11, pp. 641-667 (2015).

Multi-scale Stabilized CVFEM

- Define control volumes around each sub-cell node
- Use a second-order (bilinear) finite element approximation for n on each sub-element

$$n^h(t, \mathbf{x}) = \sum_j n_j(t) \phi_j(\mathbf{x})$$

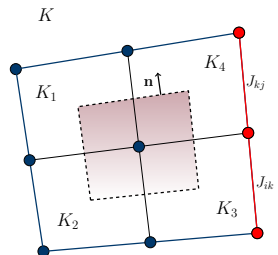


Multi-scale Stabilized CVFEM

- Define control volumes around each sub-cell node
- Use a second-order (bilinear) finite element approximation for n on each sub-element

$$n^h(t, \mathbf{x}) = \sum_j n_j(t) \phi_j(\mathbf{x})$$

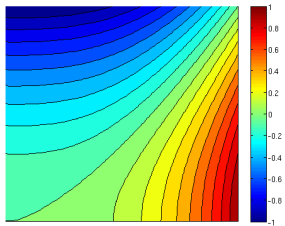
- Compute J_{ij} at each macro element edge and evaluate \mathbf{J}_E at control volume side integration points using 2nd order $H(\text{curl})$ basis



Manufactured Solution

$$\begin{aligned} -\nabla \cdot \mathbf{J}(n) &= R && \text{in } \Omega \\ \mathbf{J}(n) &= (D\nabla n + \mu\mathbf{E}n) && \text{in } \Omega \\ n &= g && \text{on } \Gamma \end{aligned}$$

$$\begin{aligned} n(x, y) &= x^3 - y^2 \\ \mu\mathbf{E} &= (-\sin \pi/6, \cos \pi/6) \end{aligned}$$



	CVFEM-MS		CVFEM-SG		FEM-SUPG	
	L^2 error	H^1 error	L^2 error	H^1 error	L^2 error	H^1 error
Grid*			$\epsilon = 1 \times 10^{-3}$			
32	1.57e-3	6.05e-2	4.24e-3	7.48e-2	2.09e-4	3.61e-2
64	3.93e-4	2.89e-2	2.07e-3	4.91e-2	4.85e-5	1.80e-2
128	8.98e-5	1.24e-2	9.78e-4	3.07e-2	1.11e-5	9.02e-3
Rate	2.06	1.14	1.06	0.642	2.12	1.00
Grid			$\epsilon = 1 \times 10^{-5}$			
32	1.69e-3	6.60e-2	4.73e-3	7.90e-2	2.30e-4	3.61e-2
64	4.54e-4	3.45e-2	2.52e-3	5.48e-2	5.78e-5	1.80e-2
128	1.18e-4	1.76e-2	1.30e-3	3.83e-2	1.45e-5	9.02e-3
Rate	1.92	0.955	0.933	0.521	1.99	1.00

* For CVFEM-MS the size corresponds sub-elements rather than macro-elements.

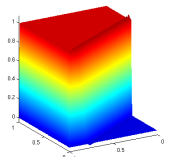
Skew Advection Test

$$\begin{aligned} -\nabla \cdot \mathbf{J}(n) &= R && \text{in } \Omega \\ \mathbf{J}(n) &= (D\nabla n + \mu\mathbf{E}n) && \text{in } \Omega \\ n &= g && \text{on } \Gamma \end{aligned}$$

$$g = \begin{cases} 0 & \text{on } \Gamma_L \cup \Gamma_T \cup (\Gamma_B \cap \{x \leq 0.5\}) \\ 1 & \text{on } \Gamma_R \cup (\Gamma_B \cap \{x > 0.5\}) \end{cases}$$

$$\mu\mathbf{E} = (-\sin \pi/6, \cos \pi/6) \quad D = 1.0 \times 10^{-5}$$

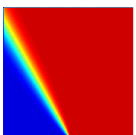
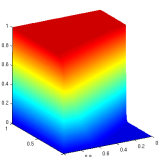
CVFEM-MS



min = -0.0445

max = 1.077

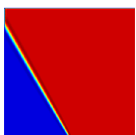
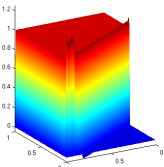
CVFEM-SG



min = 0.00

max = 1.004

SUPG



min = -0.0459

max = 1.251

Double Glazing Test

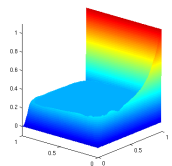
$$\begin{aligned} -\nabla \cdot J(n) &= R && \text{in } \Omega \\ J(n) &= (D\nabla n + \mu \mathbf{E} n) && \text{in } \Omega \\ n &= g && \text{on } \Gamma \end{aligned}$$

$$D = 1.0 \times 10^{-5}$$

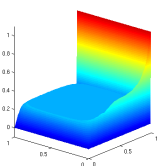
$$g = \begin{cases} 0 & \text{on } \Gamma_L \cup \Gamma_T \cup (\Gamma_B \cap \{x \leq 0.5\}) \\ 1 & \text{on } \Gamma_R \cup (\Gamma_B \cap \{x > 0.5\}) \end{cases}$$

$$\mu \mathbf{E} = \begin{pmatrix} 2(2y-1)(1-(2x-1)^2) \\ -2(2x-1)(1-(2y-1)^2) \end{pmatrix}$$

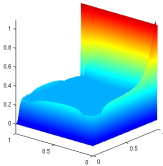
CVFEM-MS



CVFEM-SG



SUPG



Conclusions

Stabilization using an edge-element lifting of classical S-G fluxes offers a stable and robust method for solving drift-diffusion equations

- Works on unstructured grids
- Does not require heuristic stabilization parameters
- Although not provably monotone, violations of solution bounds are less than for a comparable scheme with SUPG stabilization
- Future work
 - Implementation of 2nd-order scheme in Charon
 - More detailed comparison of methods for full drift-diffusion equations